Elucidation of the Mechanism of Selenoprotein Glutathione Peroxidase (GPx)-Catalyzed Hydrogen Peroxide Reduction by Two Glutathione Molecules: A Density Functional Study†

Rajeev Prabhakar,‡ Thom Vreven,§ Keiji Morokuma,*,‡ and Djamaladdin G. Musaev*,‡

Cherry L. Emerson Center for Scientific Computation and Department of Chemistry, Emory University, 1515 Dickey Drive, Atlanta, Georgia 30322, and Gaussian, Incorporated, 340 Quinnipiac Street, Building 40, Wallingford, Connecticut 06492

Received May 3, 2005; Revised Manuscript Received June 10, 2005

ABSTRACT: The mechanism of the hydrogen peroxide reduction by two molecules of glutathione catalyzed by the selenoprotein glutatione peroxidase (GPx) has been computationally studied. It has been shown that the first elementary reaction of this process, (E-SeH) + H_2O_2 → (E-SeOH) + H_2O (1), proceeds via a stepwise pathway with the overall barrier of 17.1 kcal/mol, which is in good agreement with the experimental barrier of 14.9 kcal/mol. During reaction 1, the Gln83 residue has been found to play a key role as a proton acceptor, which is consistent with experiments. The second elementary reaction, (E-SeOH) + GSH → (E-Se-SG) + HOH (2), proceeds with the barrier of 17.9 kcal/mol. The last elementary reaction, (E-Se-SG) + GSH → (E-SeH) + GS-SG (3), is initiated with the coordination of the second glutathione molecule. The calculations clearly suggest that the amide backbone of the Gly50 residue directly participates in this reaction and the presence of two water molecules is absolutely vital for the reaction to occur. This reaction proceeds with the barrier of 21.5 kcal/mol and is suggested to be a rate-determining step of the entire GPx-catalyzed reaction H_2O_2 + 2GSH → GS-SG + $2H_2O$. The results discussed in the present study provide intricate details of every step of the catalytic mechanism of the GPx enzyme and are in good general agreement with experimental findings and suggestions.

Since the discovery of the trace element selenium (Se) in 1817, the selenium research related to mammalian biochemistry has made tremendous progress. The essentiality of this compound for mammals is evident from the fact that a poor selenium status has been associated with many deadly diseases such as cancer, HIV, cardiovascular, and Keshan−Back (*1*, *2*). In the last 2 decades, selenoenzymes have been a subject of intensive research activity (*3*). Special attention has been paid to understand and mimic the activity of the selenoprotein glutathione peroxidase (GPx),[1] which demonstrates a strong antioxidant activity and protects cell membranes and other cellular components against oxidative damage (*4*, *5*). The present density functional study is another step in this direction in which the catalytic mechanism of GPx has been investigated at the atomic level. GPx reduces numerous reactive oxygen species (ROS) like hydrogen peroxide and almost every hydroperoxide including lipid hydroperoxides by utilizing various reducing substrates (*4*). Four different classes of Se-dependent GPx: (1) cytosolic (GPx-1), (2) gastrointestinal tract (GPx-2), (3) extracellular (GPx-3), and (4) phospholipid hydroperoxide (GPx-4) have been classified (*3*). All four types of GPx are easily reduced by glutathione (GSH), while they also accept some other reducing substrates. For example, GPx-3 can be reduced by glutaredoxin and thioredoxin (*6*), and GPx-4 utilizes protein thiols as reducing substrates (*7*, *8*).

The crystal structures of only bovine erythrocyte (intracellular enzyme, GPx-1) and human plasma (extracellular enzyme, GPx-3) GPx have been resolved at 2.0 and 2.9 Å resolutions, respectively (*9*, *10*). These studies show that enzymes are tetramers, with two asymmetric units containing two dimers. Each of the dimers has two selenocysteine residues at their active sites. The overall active-site structures of both enzymes are very similar, while the environments around their selenocysteine residues are quite different. Only half of the residues at the active site within a range of 10 Å are conserved in both enzymes (*10*). The occurrence of a selenocysteine residue is the most peculiar feature of the active site of GPx. The following experimental observations explicitly implicate the selenocysteine residue in the catalytic cycle: (1) The treatment of the oxidized enzyme with cyanide destroys the catalytic activity and releases selenium from the enzyme (*11*). (2) Iodoacetate inhibits only the substrate-reduced enzyme and reacts with the selenocysteine residue (*12*). (3) A photoelectron spectroscopic study shows that the redox state of selenium in GPx depends on the substrate present (*13*). (4) In the crystalline state, the selenium sites of the oxidized enzyme can be reduced (*14*). (5) The formation of the E-Se-S-G complex through selenosulfide linkage has recently been demonstrated (*15*).

† This research was supported by a grant from the National Science Foundation (CHE-0209660).

* To whom correspondence should be addressed. E-mail: dmusaev@emory.edu. Telephone: 404-727-2382. Fax: 404-727-7412.

‡ Emory University.

§ Gaussian, Inc.

[1] Abbreviations: GPx, glutathione peroxidase; GSH, glutathione; DFT, density functional theory; TS, transition state.

10.1021/bi050815q CCC: $30.25
Published on Web 08/09/2005

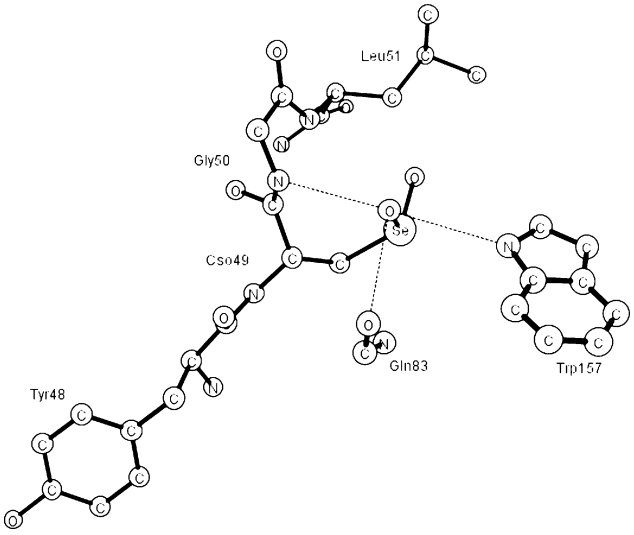

FIGURE 1: X-ray structure of the active-site region of GPx.

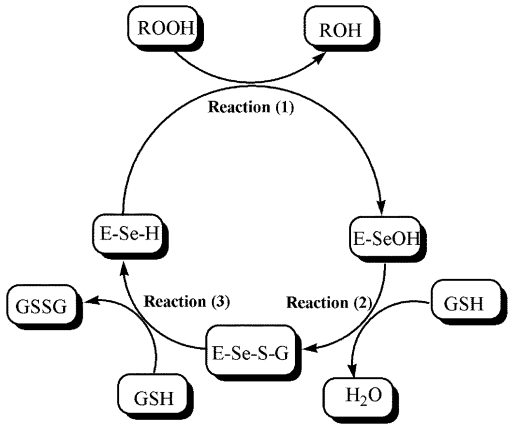

FIGURE 2: Experimentally suggested mechanism for the catalytic cycle of GPx.

The X-ray structure of the active site of human plasma GPx is shown in Figure 1. As shown in this figure, the selenocysteine residue of the enzyme exists in the "resting" seleninic acid, E-Se(O)(OH), form. The active-site Gln83 and Trp157 residues are located within hydrogen-bonding distance to the selenium atom and have been suggested to play a critical role in the catalysis (*9*). These two residues are known to be conserved in the entire GSH superfamily and their homologues, which probably account for the similarities in their catalytic mechanism (*16*). The active-site seleninic acid residue is coordinated to Gly50 and Tyr48 in a tetradic arrangement (*10*). Aforementioned features of active site of GPx have been mimicked in various organoselenium compounds possessing a direct Se−N bond, and the most prominent among them is an anti-inflammatory drug called Ebselen (*17*−*19*).

Biochemical (*5*), kinetic (*20*), and crystallographic (*9*) studies on the bovine cellular enzyme have suggested that the selenocysteine residue directly participates in the catalytic process of reduction of hydroperoxide by GPx. It has been experimentally suggested that the catalytically active form of the enzyme is either selenolate anion (E-Se^-) or selenol (E-SeH) (*9*). The proposed mechanism of the overall catalytic cycle is shown in Figure 2. In the first step, reaction 1,

hydrogen peroxide reduction is accompanied by the oxidation of the selenolate anion (or selenol) to the selenenic acid. The experimental measure rate for this reaction of 0.51 s^{-1} corresponds to a barrier of 14.9 kcal/mol (*21*). In the second step, reaction 2, the formed selenenic acid subsequently reacts with the substrate GSH to produce seleno-sulfide adduct (E-Se-SG), which has been observed recently (*15*). In the third step, reaction 3, a second molecule of GSH attacks the seleno-sulfide adduct to regenerate the active form of the enzyme and forms disulfide GS-SG. This step has been suggested to be a rate-determining step of the entire mechanism (*22*). Thus, in the full catalytic cycle, 2 equiv of GSH are consumed to produce the disulfide and water.

Despite the availability of the above-detailed experimental information, the catalytic mechanism of the GPx enzyme and the factors controlling its activity are not known with certainty. The high-level quantum chemical approaches incorporating all of the available experimental information can make significant contributions toward the deeper understanding of the mechanism of this critical enzyme. The calculations performed in the present paper not only allow for a detailed study of individual steps of the mechanism but also provide energetics and structures of all short-lived intermediates and transition states (TSs).

II. COMPUTATIONAL DETAILS

A. Methods. All calculations were performed using the Gaussian 03 program (*23*). The geometries of the reactants, intermediates, TSs, and products were optimized without any symmetry constraints using the B3LYP method (*24*) and 6-31G(d) basis set. All degrees of freedom were optimized, and the TSs obtained were confirmed to have one imaginary frequency corresponding to the reaction coordinate. The final energetics of the optimized structures were improved by performing single-point calculations using a triple-ζ quality basis set 6-311+G(d,p). Because it was computationally unfeasible to calculate unscaled zero-point energy and thermal corrections using triple-ζ quality basis set, these effects are estimated at the B3LYP/6-31G(d) level and added to the final B3LYP/6-311+G(d,p) energetics. This type of correction is an adequate approximation and has commonly been used in quantum chemical studies (*25*). The suggested mechanism of the GPx involves H_2O_2 and two GSH molecules, which consecutively enter the active site and participate in the catalytic reactions. Their exact binding sites prior to the participation in reactions are not known, and there is a large difference in the entropy contribution from the binding of an absolutely free and a prebonded molecule. Because it is not possible to calculate reliable entropic contributions without knowing their binding states, they are assumed to be "free"; therefore, the entropy effects are not included in the final energetics.

The dielectric effects from the surrounding environment were estimated using the self-consistent reaction field IEF−PCM method (*26*) at the B3LYP/6-31G(d) level. These calculations were performed with a dielectric constant of 4.3 corresponding to diethyl ether, close to 4.0 generally used to describe the protein surrounding.

Throughout the paper, the energies obtained at the B3LYP/(6-311+G(d,p)) + zero-point vibrational and thermal corrections (at 298.15 K and 1 atm) + solvent effects (at B3LYP/6-31G(d) level) are used, while the energies without the solvent effects are provided in parentheses. In the figures,

for the sake of clarity, the complete models used in the calculations are shown only for transition-state structures.

B. Models. Experimental studies on bovine erythrocyte GPx have suggested a half-site reactivity of the enzyme, i.e., that two GSH molecules bind to each tetramer (*9*), which justifies the use of a monomer to study the enzyme reactivity. Here, the first question to be considered concerns the choice of an appropriate model for the enzyme active site that retains all of its basic features. Because the selenocysteine residue is experimentally suggested to play a critical role in the catalytic cycle (*11*−*15*), it is included in the model. The active-site Gln83 and Trp157 residues, known to be conserved in all known GPx's and experimentally suggested to be involved in the catalytic mechanism (*9*), are also included in the model. In addition, in the X-ray structure (*10*), Tyr48, Gly50, and Leu51 residues are shown to form a part of the cage around the selenocysteine residue; therefore, they are also included in the model. In the first and third step of the mechanism, one and two water molecules, respectively, are also included into the active-site model. On the basis of the earlier experience, glutamine and tryptophan residues are modeled by formamide and indole, respectively.

The next question deals with the active state of the enzyme. According to experiments, in the active state of the enzyme, the selenocysteine residue could be either in the selenolate anion (E-Se^-) or selenol (E-SeH) form. B3LYP calculations show that the (E-SeH + Gln83) arrangement is 10.0 kcal/mol more favorable than the (E-Se^- + $Gln83^+$), justifying the use of the selenol (E-SeH) form of the enzyme as a starting point in our studies.

In the X-ray structure (*10*), the side chain of the Gln83 residue is positioned perpendicular to the side chains of selenocysteine and Trp157 residues, which during the optimization could lead to two different conformers corresponding to the facing of either oxo or $-NH_2$ group of Gln83 toward Trp157. The density functional theory (DFT) calculations suggest that these conformers have nearly the same energies. However, the former is more consistent with the experimentally suggested role of Gln83 and therefore used in the present study. The overall charge of the model is chosen to be zero. The substrate GSH (γ-glutamylcysteinylglycine, γ-GluCysGly) is a tripeptide and forms a peptide bond through the γ-carboxyl group rather than the normal α-carboxyl group. In this study, it has been modeled by ethanethiol, C_2H_5SH.

The models used in the present study are truncated from the X-ray structure. However, it has to be mentioned that no geometrical constraint has been imposed and during optimization noncontiguous residues such as Gln83 and Trp157 do not drift apart and largely remain at their hydrogen-bond-donating positions.

III. RESULTS AND DISCUSSION

The experimentally suggested mechanism, shown in Figure 2, was used as a starting point for the present study. The overall reaction investigated in this study

$$HOOH + 2C_2H_5SH \rightarrow C_2H_5S-SC_2H_5 + 2H_2O$$

is calculated to be exothermic by 73.0 (69.0) kcal/mol.

A. Mechanism of Reaction 1: Conversion of Selenol to Selenenic Acid by Hydrogen Peroxide. Hydrogen Peroxide Coordination. Because the active site of the GPx enzyme has previously been suggested to have water molecules (*27*), the present step of the reaction has been investigated with and without the presence of a water molecule in the active site. For brevity, we show only structures with a water molecule in Figures 3 and 4. In the first step of this reaction, the hydrogen peroxide molecule coordinates to the active site of the enzyme (structure **I**) to give structure **II**. In **II**, the H_2O_2 molecule binds to the active site by forming strong hydrogen bonds with the water molecule and the Gly50 residue. In **II**, the water molecule retains hydrogen bonds to the selenol SeH and Gln83 residues. The binding energy of a *free* hydrogen peroxide is calculated to be 6.3 (13.5) kcal/mol. In the absence of a water molecule, H_2O_2 forms hydrogen bonds with the selenol and Gly50 and Gln83 residues and the calculated binding energy is reduced by 1.0 kcal/mol.

The next step of reaction 1 is the formation of selenenic acid. In general, this step could occur by either a stepwise or concerted mechanism. The stepwise mechanism consists of two parts: (a) formation of selenolate anion (E-Se^-) and (b) O−O bond cleavage.

Stepwise Mechanism of Formation of Selenenic Acid: Part 1. Formation of Selenolate Anion (E-Se^-). During the first part of the stepwise mechanism, the Se−H bond of the selenol (R-Se^-) is broken and simultaneously the proton is transferred through the oxygen atom of hydrogen peroxide and a water molecule to the neighboring Gln83, providing an intermediate product **III** (see Figure 3) in which the selenolate anion (R-Se^-) and protonated Gln83 are formed. The optimized transition-state (TS) structure (**TS**−**II**−**III**, Figure 3) has a hydrogen-bond network from Gly50 and Trp157 residues, which helps to stabilize the TS. The computed barrier for this step is 12.8 (14.6) kcal/mol, which could be slightly overestimated because B3LYP is known to overestimate the activation energy for long-range proton-transfer reactions (*28*). This step is calculated to be endothermic by 9.5 (11.9) kcal/mol. In the intermediate **III**, confirmed to be a minimum by normal coordinate analysis, the O−H bond of 1.1 Å in protonated Gln83 seems to be slightly longer than the normal (0.98 Å) O−H bond. The model without the active-site water molecule increases the barrier slightly (∼1.0 kcal/mol) and also the endothermicity by 1.1 kcal/mol.

Thus, the present calculations suggest that the Gln83 residue plays a key role of a proton acceptor, which is consistent with the available experimental suggestion that the Gln83 residue participates in the catalytic cycle (*9*).

Stepwise Mechanism of Formation of Selenenic Acid: Part 2. O−O Bond Cleavage. In the second part of the stepwise pathway of E-SeOH formation, the O−O bond of H_2O_2 is cleaved and the hydroxyl of H_2O_2 is transferred to the selenolae anion (E-Se^-). In this part, the proton previously transferred to the Gln83 residue moves to the terminal oxygen atom of H_2O_2 and cleaves the O−O bond, forming selenenic acid and a water molecule (**IV**). The optimized TS (**TS**−**III**−**IV**) for this process (see Figure 3) indicates that this step is synchronous; i.e., all bonds distances change smoothly from the reactant **III** to the product **IV**. The barrier for this process is 7.6 (8.5) kcal/mol, making the overall barrier (from **II** to **IV**) for the formation of the selenenic acid (E-Se-OH)

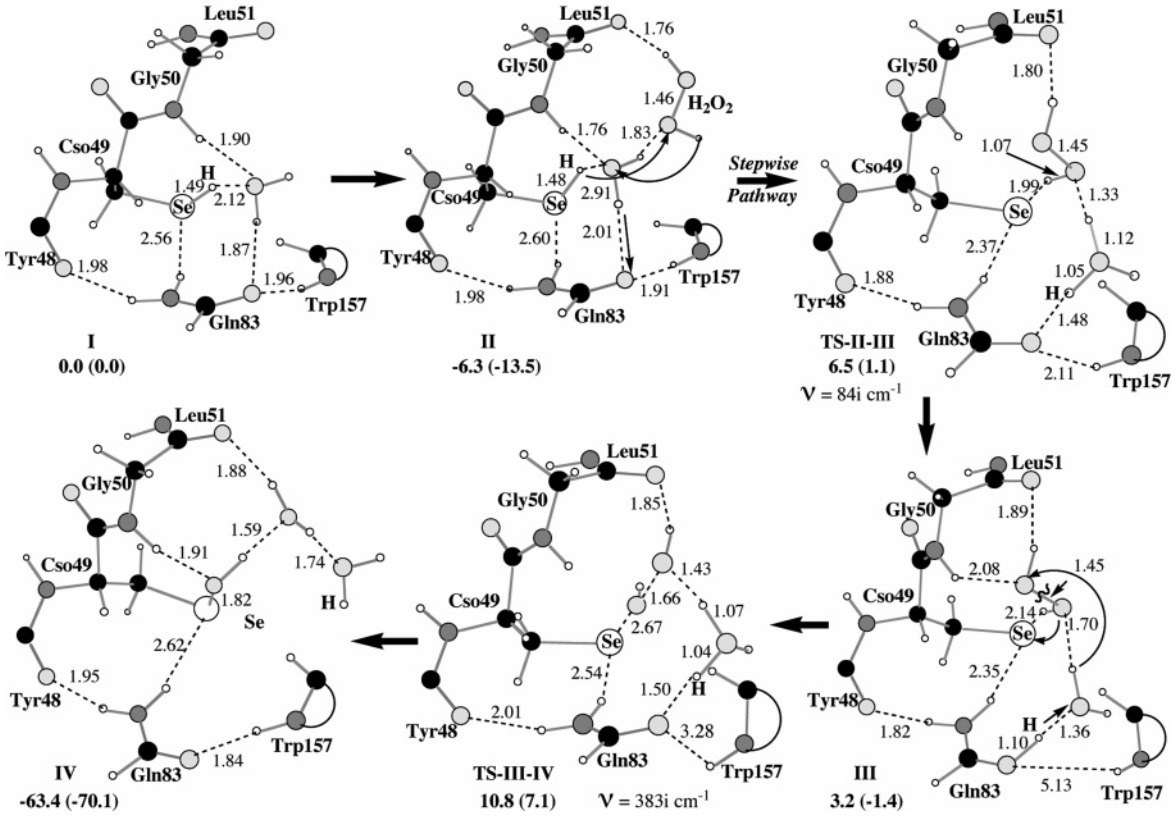

FIGURE 3: Optimized structures (in Å) and energies [with and without (in parentheses) solvent effects, in kcal/mol] of the reactant, intermediates and, TSs for the stepwise mechanism of reaction 1.

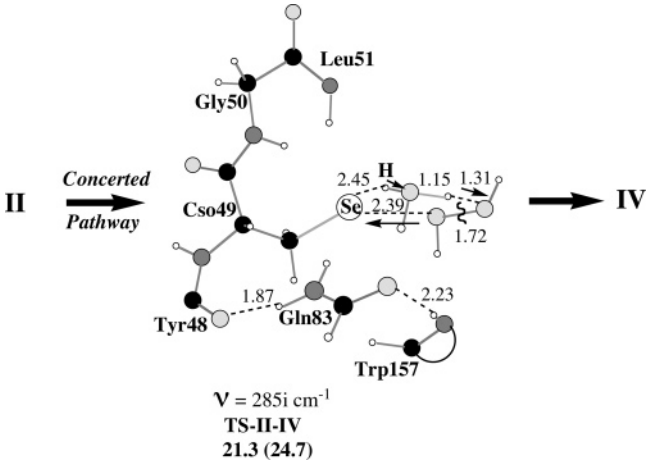

FIGURE 4: Optimized structures (in Å) and energies [with and without (in parentheses) solvent effects, in kcal/mol] of the reactant, intermediates, and TSs for the concerted mechanism of reaction 2.

17.1 (20.6) kcal/mol. The absence of a water molecule in the active-site model increases the barrier by 2.0 kcal/mol. These calculated barriers are in excellent agreement with the experimentally measured barrier of 14.9 kcal/mol (*21*). This step of reaction 1 is calculated to be exothermic by 66.6 (69.7) kcal/mol.

It is noteworthy that we have explored many other pathways to achieve the O−O bond cleavage. In one such pathway, a proton transfer from the protonated Gln83 to the oxygen of H_2O_2 accompanied by an intramolecular proton transfer between oxygen atoms of H_2O_2 raises the activation barrier by 4.9 kcal/mol. In another attempt, the activation of the water molecule accompanied by simultaneous proton transfers from the protonated Gln83 and water molecule to the H_2O_2 leading to the O−O bond cleavage increases the barrier by 6.1 kcal/mol.

Concerted Mechanism of Reaction 1. The reaction could also follow a concerted pathway. In this pathway, the formation of selenenic acid occurs in a single step, where the water molecule included in the active-site model plays the role of a bridge between the proton donor and acceptor sites. The optimized TS **TS−II−IV** is shown in Figure 4. During this process, the Se−H bond of the selenol (E-SeH) is broken, and with the help of the bridging water molecule, a proton is transferred to H_2O_2, which in turn cleaves the O−O bond of H_2O_2 and produces a ESe−OH bond. Also, it is noteworthy that the concerted pathway does not involve the Gln83 residue in the process, which is not in line with the experimental suggestion (*9*). The computed reaction barrier for this concerted mechanism is 4.2 kcal/mol higher than that for the stepwise mechanism discussed above. In the absence of a water molecule, this barrier is further increased by 4.1 kcal/mol. Because the barrier for the concerted mechanism is substantially higher than that for the stepwise mechanism, this mechanism is ruled out.

B. Mechanism of Reaction 2: Formation of the Seleno-sulfide Adduct. As shown in Figure 5, reaction 2 starts with the coordination of the first *unbound* GSH molecule to the selenenic acid (**IV**) leading to the formation of the selenenic acid−GSH complex (**V**), with the (E-SeOH)−(GSH) binding energy of only 4.2 (7.5) kcal/mol. Because the water molecule formed in the previous step does not participate in this reaction, it is excluded from the model. From the weakly bound complex **V**, the reaction proceeds through the TS (**TS−V−VI**) and produces the seleno-sulfide adduct and a water molecule (**VI**). At the TS, synchronously, the S−H

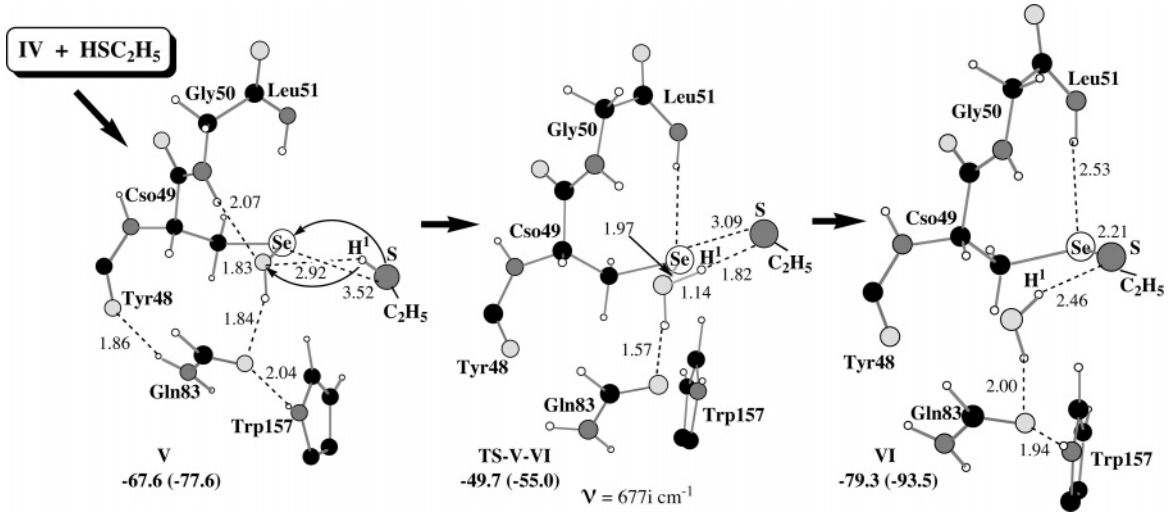

FIGURE 5: Optimized structures (in Å) and energies [with and without (in parentheses) solvent effects, in kcal/mol] of the reactant, intermediates, and TSs for reaction 2.

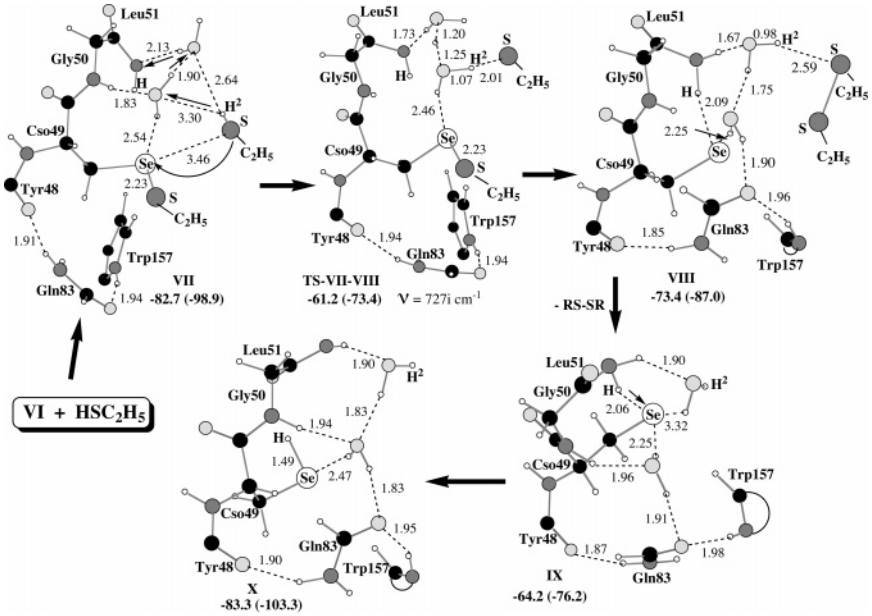

FIGURE 6: Optimized structures (in Å) and energies [with and without (in parentheses) solvent effects, in kcal/mol] of the reactant, intermediates, and TSs for reaction 3.

bond of the GSH is broken and a proton is transferred to the hydroxyl group of the selenenic acid accompanied by the formation of a Se−S bond. The barrier for this step is calculated to be 17.9 (22.6) kcal/mol, and the reaction is exothermic by 15.9 (23.4) kcal/mol. It should be mentioned that the formation of the seleno-sulfide adduct (E-Se-SG) through selenosulfide linkage has been observed experimentally (*15*).

C. Mechanism of Reaction 3: Formation of Disulfide and Regeneration of Selenol. As shown in Figure 6, the final step of the GPx mechanism is reaction 3, where the second GSH molecule reacts with the seleno-sulfide adduct (**VI**) to produce the selenol (E-SeH) and oxidized disulfide (GS-SG) form of GSH (**X**). This is the most critical and complex step of the entire mechanism and is experimentally suggested to be the rate-limiting step (*22*). In the present study, we have explored several different pathways for this reaction before suggesting the most plausible one. As expected, the first process of all possible pathways is the coordination of *free* GSH to the seleno-sulfide adduct to form a weekly bound (E-Se-SC_2H_5)(C_2H_5SH) complex (**VII**). The (E-Se-SC_2H_5)−(C_2H_5SH) binding energy is found to be only 3.4 (5.4) kcal/mol.

Concerted Mechanism. From the complex **VII**, reaction 3 may proceed via different pathways. The most straightforward pathway is a concerted one, involving simultaneous cleavage of the S−H bond of the substrate and the formation of the Se−H and the disulfide (S−S) bonds. In the absence of any water molecule in the active site, the concerted TS (see the Supporting Information) connecting the reactants (E-Se-SR + C_2H_5SH) directly to the final products (E-SeH + $C_2H_5S-SC_2H_5$) is prohibitively high in energy, ca. 50 kcal/mol. The inclusion of one water molecule leads to the formation of H_3O^+ species at the TS and reduces this barrier only by 8.0 kcal/mol. Ideally, it could be expected that the addition of another water molecule will lead to the formation of $O_2H_5^+$ species and significantly reduce the barrier. However, in the presence of two water molecules, all attempts to achieve the concerted TS failed because the proton always tends to move toward the backbone of the

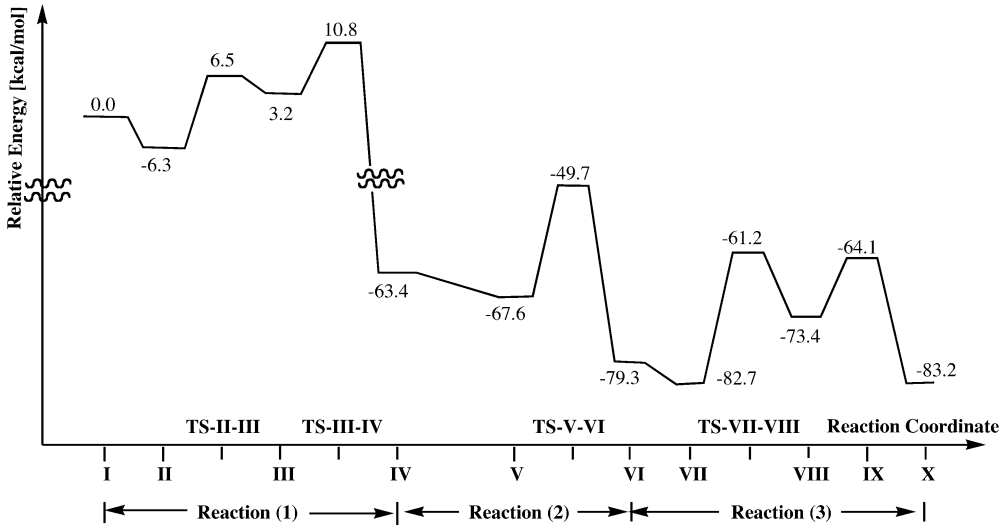

FIGURE 7: Energy diagram for the catalytic mechanism of GPx (including solvent effects).

Gly50 residue. Furthermore, all of the efforts to find the product involving the formation of $O_2H_5^+$ species rather than the protonated Gly50 residue were unsuccessful. The major reason for these failures was a lower barrier for the backward reaction, which causes $O_2H_5^+$ species to immediately donate a proton to the substrate, and the system goes back to the reactant. Even upon optimizing in the presence of the solvent protein using the polarized continuum model (PCM) method (*26*), the $O_2H_5^+$ species could not be stabilized. One may conclude that in the presence of two water molecules the concerted reaction pathway does not exist.

On the basis of the above-discussed results, it is concluded that regardless of the presence of water molecule(s) the concerted mechanism is not possible because of the high barrier or the nonexistence of the pathway.

Stepwise Mechanism. Therefore, we have investigated in detail the stepwise pathway in the presence of two water molecules. As shown in Figure 6, we found a pathway via **TS**−**VII**−**VIII**, in which the S−H bond of the GSH is cleaved with the simultaneous transfer of the proton via two water molecules to the amide backbone of Gly50. It has to be noted that these two water molecules are required to bridge the proton donor (GSH) and acceptor (Gly50) sites. This process leads to the formation of the oxidized form **VIII** of GSH $C_2H_5S-SC_2H_5$ and the protonated Gly50 residue. The calculated barrier is calculated to be 21.5 (25.5) kcal/mol; thus, this step of the reaction is a rate-determining step of the entire catalytic cycle (reaction 4). This is in agreement with the experiments (*22*). However, in this step, also a long-range proton transfer takes place, the barrier of which could be overestimated by DFT (*28*). The formed product (**VIII**) could be described as a weakly bound complex where the selenocysteine residue is in the selenolate (E-Se^-) form. The formation of this product is calculated to be endothermic by 9.3 (11.9) kcal/mol.

Thus, from the aforementioned results, it is evident that the amide backbone of Gly50 participates directly in the reaction. To our knowledge, there is no precedence indicating such a mechanism, and this proposal is suggested on the basis of its energetic feasibility after investigating all of the other possibilities on the model system. However, it has to be mentioned that the utilization of the amide backbone is not a unique feature of this enzyme. In several other enzymes, for example, Ni-containing superoxide dismutase (Ni−SOD) amino acid residues have been experimentally proposed to donate protons from their amide backbones (*29*).

Other Possible Pathways. In addition to the stepwise mechanism discussed above, an oxidative addition pathway leading the formation of a tetracoordinated selenium species [E-Se(H)(SG)(SG)] has also been investigated (see the Supporting Information). The calculations suggest that this species is 20.0 kcal/mol higher in energy than **VIII**; therefore, it is unlikely to be formed.

After the GS−H bond cleavage, one could also expect the existence of the [(E-Se-SG)(SG^-)($Gly50^+$)] complex on the potential energy surface of the reaction. However, our extensive search to locate this minimum has shown that this structure does not exist in the gas phase and optimization converges to the [(E-Se^-)($Gly50^+$)(GS-SG)] complex (**VIII**). It is possible that this minimum exists in the presence of the surrounding protein and is under investigation.

Regeneration of Selenol. After the formation of [(E-Se^-)-($Gly50^+$)(GS-SG)] intermediate (**VIII**), the reaction proceeds via an abstraction of a proton from the protonated Gly50 by the selenolate ion (see Figure 6). Because the $C_2H_5S-SC_2H_5$ species is not expected to participate in this part of the mechanism, it is left out in the model of the product **IX**. Calculations show that this process occurs with a very small barrier, which we failed to locate. However, this small barrier does not affect the suggested mechanism of the reaction. This process is driven by a strong exothermicity of 19.1 (27.1) kcal/mol. In the product **X**, the selenol and neutral Gly50 are formed and the enzyme returns to its original form for the next catalytic cycle.

D. Reaction Mechanism of the Entire Catalytic Cycle. The energy diagram of the studied reaction

$$[\text{E-SeH}](H_2O) + \text{HOOH} + 2\text{RSH} \rightarrow [\text{E-SeH}](H_2O)_2 + \text{RS-SR} + H_2O$$

is shown in Figure 7. From this figure, it is clear that the GPx-catalyzed hydrogen H_2O_2 reduction by two molecules of thiol includes three elementary reactions, as proposed experimentally.

In the first reaction 1, the active selenol (E-SeH) form of GPx uptakes the hydrogen peroxide molecule and produces selenenic acid (E-SeOH) and a water molecule. The first step of the reaction 1 is the coordination of the hydrogen peroxide molecule to the active-site selenol (E-SeH) state of the enzyme to form complex **II**. This process is found to be exothermic by 6.3 (13.5) kcal/mol. From the resulted complex **II**, the reaction is suggested to proceed via a stepwise pathway, which is divided into two parts: (a) a proton transfer from the (E-SeH) to Gln83 residue through a hydrogen peroxide and a water molecule leading to the formation of (E-Se^-) and protonated Gln83 (**III**) and (b) the O−O bond cleavage via protonating the terminal oxygen atom of H_2O_2 by the proton earlier transferred to the Gln83 residue. As a result, a water molecule and selenenic acid (**IV**) are formed. The DFT calculations show that the first part of this stepwise pathway occurs through the TS **TS**−**II**−**III** with a 12.8 (14.6) kcal/mol barrier and is endothermic by 9.5 (11.9) kcal/mol. The second part of the stepwise pathway occurs with a barrier of 7.6 (8.5) kcal/mol. Because the O−O bond cleavage is followed by the formation of **III**, which is endothermic by 9.5 (11.9) kcal/mol, the overall barrier for the formation of the selenenic acid (E-SeOH), in reaction 1, becomes 17.1 (20.6) kcal/mol. The calculated barrier for the hydrogen peroxide reduction is in excellent agreement with the experimentally measured barrier of 14.9 kcal/mol (*21*). Reaction 1 is calculated to be exothermic by 63.4 (70.1) kcal/mol.

On the basis of the results obtained in the first part of this reaction, the Gln83 residue is suggested to play a key role as a proton acceptor, which is consistent with the experimental proposal indicating that the Gln83 residue participates in the catalytic cycle (*9*).

The second elementary reaction, reaction 2, starts with the coordination of the first GSH molecule to the previously formed selenenic acid (E-SeOH) and leads to the formation of a weak selenenic acid−GSH complex (**V**). The binding energy of (E-SeOH)−(GSH) is calculated to be 4.2 (7.5) kcal/mol. The reaction proceeds further through the TS **TS**−**V**−**VI** and climbs a barrier of 17.9 (22.6) kcal/mol, corresponding to the S−H bond cleavage and a proton transfer to the hydroxyl group of the selenenic acid. In the product, seleno-sulfide adduct (E-Se-SG) and the water molecule (**VI**) are formed. Reaction 2 is calculated to be exothermic by 15.9 (23.4) kcal/mol. The formation of the E-Se-SG complex through selenosulfide linkage has been observed experimentally (*15*).

In the last elementary reaction 3 of the mechanism, the active form of the enzyme (E-SeH) is regenerated and GSH is oxidized to GS-SG by the second GSH molecule. We have explored all possible reaction pathways and demonstrated that the amide backbone of Gly50 directly participates in this process and the presence of two water molecules is absolutely necessary to bridge the proton donor (GSH) and acceptor (Gly50) sites. In this step, the S−H bond of the GSH is broken and the proton is transferred via two water molecules to the amide backbone of Gly50. This process leads to the formation of the oxidized form of GSH C_2H_5S−SC_2H_5 and the protonated Gly50 residue. The calculated barrier for this step is 21.5 (25.5) kcal/mol and corresponds to the TS **TS**−**VII**−**VIII**. This step is proposed to be a rate-determining step of the entire catalytic mechanism, which is in agreement with the experiments (*22*). The product **VIII** formed in this step could be described as a weakly bound complex, where the selenocysteine residue is in its selenolate (E-Se^-) form. Later, this product rearranges to the final product of selenol **X**, with almost no barrier. The formation of the selenol (E-SeH) is exothermic by 19.1 (27.1) kcal/mol, and the enzyme returns back to its original form.

IV. CONCLUSIONS

In the present study, the catalytic mechanism of selenoprotein GPx-catalyzed hydrogen peroxide reduction by two molecules of GSH is described by three elementary reactions.

The first elementary reaction, (E-SeH) + H_2O_2 → (E-SeOH) + H_2O (1), is found to proceed via a stepwise pathway with the overall barrier of 17.1 (20.6) kcal/mol, which is in good agreement with the experimentally measured barrier of 14.9 kcal/mol (*21*). It is demonstrated that the Gln83 residue plays a key role as a proton acceptor during reaction 1. The second elementary reaction, (E-SeOH) + GSH → (E-Se-SG) + HOH (2), proceeds with a barrier of 17.9 (22.6) kcal/mol. However, as suggested experimentally (*22*), the rate-determining step of the entire GPx-catalyzed reaction H_2O_2 + 2GSH → GS-SG + $2H_2O$ is found to be the third and last elementary reaction, (E-Se-SG) + GSH → (E-SeH) + GS-SG (3), which proceeds with the barrier of 21.5 (25.5) kcal/mol. Our results clearly show that the amide backbone of the Gly50 residue participates directly in this reaction and the presence of two water molecules is absolutely vital for the reaction to occur. The model calculations performed in the present study have provided aforementioned invaluable insights in the complex mechanism of this remarkable enzyme.

ACKNOWLEDGMENT

A DURIP Grant (FA9550-04-1-0321) from AFOSR is also acknowledged for support of the computer facilities. The use of computational resources at the Cherry Emerson Center for Scientific Computation is also acknowledged.

SUPPORTING INFORMATION AVAILABLE

(a) Complete ref *28*; (b) Tables S1−S7, Cartesian coordinates (in Å) of all of the optimized structures including TSs for reaction 1; (c) Tables S8−S10, Cartesian coordinates (in Å) of all of the optimized structures including TSs for reaction 2; and (d) Tables S11−S17, Cartesian coordinates (in Å) of all of the optimized structures including TSs for reaction 3. This material is available free of charge via the Internet at http://pubs.acs.org.

REFERENCES

1. Combs, G. F., Jr., and Lü, J. (2001) *Selenium Its Molecular Biology and Role in Human Health* (Hatfield, D. L., Ed.) p 205, Kluwer Academic Publishers, Boston, MA.
2. Zhao, L., Cox, A. G., Ruzicka, J. A., Bhat, A. A., Zhang, W., and Taylor, E. W. (2000) Molecular modeling and *in vitro* activity of an HIV-1-encoded glutathione peroxidase, *Proc. Natl. Acad. Sci. U.S.A. 97*, 6356.
3. Birringer, M., Pilawa, S., and Flohè, L. (2002) Trends in selenium chemistry, *Nat. Prod. Rep. 19*, 693−718.
4. Mills, G. C. (1957) Hemoglobin catabolism. I. Glutathione peroxidase, an erythrocyte enzyme which protects hemoglobin from oxidative breakdown, *J. Biol. Chem. 229*, 189−197.

5. Flohè, L. (1989) *Glutathione* (Dolphin, D., Avramovic, O., and Poulson, R., Eds.) pp 644−731, John Wiley and Sons, New York, 1989.
6. Björnstedt, M., Xue, J., Huang, W., Akesson, B., and Holmgren, A. (1994) The thioredoxin and glutaredoxin systems are efficient electron donors to human plasma glutathione peroxidase, *J. Biol. Chem. 269*, 29382.
7. Godeas, C., Sandri, G., and Panfili, E. (1994) Distribution of phospholipid hydroperoxide glutathione peroxidase (PHGPx) in rat testis mitochondria, *Biochim. Biophys. Acta 1191*, 147.
8. Roveri, A., Ursini, F., Flohé, L., and Maiorino, M. (2001) PHGPx and spermatogenesis, *Biofactors 14*, 213.
9. Epp, O., Ladenstein, R., and Wendel, A. (1983) The refined structure of the selenoenzyme glutathione peroxidase at 0.2-nm resolution, *Eur. J. Biochem. 133*, 51−69.
10. Ren, B., Huang, W., Åkesson, B., and Ladenstein, R. (1997) The crystal structure of seleno-glutathione peroxidase from human plasma at 2.9 Å resolution, *J. Mol. Biol. 268*, 869−885.
11. Prohaska, J. R., Oh, S. H., Hoekstra, W. G., and Ganther, H. E. (1977) Glutathione peroxidase: Inhibition by cyanide and release of selenium, *Biochem. Biophys. Res. Commun. 74*, 64−71.
12. Forstrom, J. W., Zakowski, J. J., and Tappel, A. L. (1978) Identification of the catalytic site of rat liver glutathione peroxidase as selenocysteine, *Biochemistry 17*, 2639−2644.
13. Wendel, A., Pilz, W., Ladenstein, R., Sawatzki, G., and Weser, U. (1975) Substrate-induced redox change of selenium in glutathione peroxidase studied by X-ray photoelectron spectroscopy, *Biochim. Biophys. Acta 377*, 211−215.
14. Ladenstein, R., Epp, O., Bartels, K., Jones, A., Huber, R., and Wendel, A. (1979) Structure analysis and molecular model of the selenoenzyme glutathione peroxidase at 2.8 Å resolution, *J. Mol. Biol. 134*, 199−218.
15. Kraus, R. J., and Ganther, H. E. (1980) Reaction of cyanide with glutathione peroxidase, *Biochem. Biophys. Res. Commun. 96*, 1116−1122.
16. Ursini, F., Maiorino, M., Brigelius-Flohé, R., Aumann, K. D., Roveri, A., Schomburg, D., and Flohé, L. (1995) Diversity of glutathione peroxidases, *Methods Enzymol. 252*, 38−53.
17. Sies, H., and Masumoto, H. (1997) Ebselen as a glutathione peroxidase mimic and as a scavenger of peroxynitrite, *Adv. Pharmacol. 38*, 229−246.
18. Musaev, D. G., and Hirao, K. (2003) Reactivity of [1,2-benzisotellurazol-3(2H)-one] with peroxynitrous acid: Comparison with Ebselen analogues, *J. Phys. Chem. A 107*, 9984−9990.
19. Musaev, D. G., Geletii, Y. V., Hill, C. L., and Hirao, K. (2003) Can the Ebselen derivatives catalyze the isomerization of peroxynitrite to nitrate? *J. Am. Chem. Soc. 125*, 3877−3888.
20. Flohé, L., Loschen, G., Gunzler, W. A., and Eichele, E. (1972) Glutathione peroxidase, V. The kinetic mechanism, *Hoppe-Seyler's Z. Physiol. Chem. 353*, 987−999.
21. Roy, G., Nethaji, M., Mugesh, G. (2004) Biomimetic studies on anti-thyroid drugs and thyroid hormone synthesis, *J. Am. Chem. Soc. 126*, 2712−2713.
22. Mugesh, G., du Mont, W., and Sies, H. (2001) Chemistry of biologically important synthetic organoselenium compounds, *Chem. Rev.* 101, 2125−2179.
23. Frisch, M. J. et al. (2004) *Gaussian 03 (revision C1)*, Gaussian, Inc., Pittsburgh, PA.
24. Becke, A. D. (1988) Density-functional exchange-energy approximation with correct asymptotic behavior, *Phys. Rev. A 38*, 3098−3100. (b) Lee, C., Yang, W., and Parr, R. G. (1988) Development of the Colle−Salvetti correlation energy formula into a functional of the electron density, *Phys. Rev. B 37*, 785−789. (c) Becke, A. D. J. (1993) Density-functional thermochemistry. III. The role of exact exchange, *Chem. Phys. 98*, 5648−5652.
25. Siegbahn, P. E. M., and Blomberg, M. R. A. (2000) Transition-metal systems in biochemistry studied by high-accuracy quantum chemical methods, *Chem. Rev. 100*, 421−437.
26. Cances, E., Mennucci, B., and Tomasi, J. (1997) A new integral equation formalism for the polarizable continuum model: Theoretical background and applications to isotropic and anisotropic dielectrics, *J. Chem. Phys. 107*, 3032−3041.
27. Prabhakar, R., Musaev, D. G., Khavrutskii, I. V., and Morokuma, K. (2004) Does the active site of mammalian glutathione peroxidase (GPx) contain water molecules? An ONIOM study, *J. Phys. Chem. B 108*, 12643−12645.
28. Prabhakar, R., Blomberg, M. R. A., and Siegbahn, P. E. M. (2000) A density functional theory study of a concerted mechanism for proton exchange between amino acid side chains and water, *Theor. Chem. Acc. 104*, 461−470.
29. Barondeau, D. P., Kassmann, C. J., Bruns, C. K., Tainer, J. A., and Getzoff, E. D. (2004) Nickel superoxide dismutase structure and mechanism, *Biochemistry 43*, 8038−8047.

BI050815Q